Beyond "Greenflation": Heterogeneous Price Dynamics in Critical Mineral Markets

Lorenzo Marcelino[†, a]
Karine Teixeira Borri[‡, a]
Diego Mesa Pena[*, b]
Pablo Brito-Parada[**, b]

[a]University of São Paulo (USP), Luiz de Queiroz College of Agriculture (ESALQ)
[b]Imperial College London, Department of Earth Science and Engineering

Abstract

The transition to low-carbon technologies is precipitating a structural shift in global commodity markets, replacing fossil fuel intensity with critical mineral intensity. This study investigates the heterogeneous transmission mechanisms of energy transition shocks in the United States copper and Chinese lithium markets, employing a Structural Vector Autoregression identified via Non-Gaussian Maximum Likelihood (NGML). By exploiting the heavy-tailed distributions of commodity shocks, we achieve data-driven identification without imposing arbitrary recursive restrictions. Our empirical results reveal a profound structural dichotomy. In the US, copper behaves as a mature, financialized upstream commodity, primarily driven by cost-push factors rather than short-term downstream renewable demand. Conversely, the Chinese lithium market exhibits pronounced structural inertia and counter-intuitive negative price response to renewable energy shocks, attributed to state-mediated policy forward guidance. These findings challenge the prevailing narrative of uniform greenflation effect, demonstrating that institutional frameworks and state interventions fundamentally alter how critical minerals price the energy transition.

Keywords: Energy transition; Critical minerals; Greenflation; Structural Vector Autoregression; Non-Gaussian Maximum Likelihood; Policy forward guidance.

JEL codes: Q02, Q42, F51, C32.

How to cite: Marcelino, L., Borri, K.T., Mesa Pena, D. & Brito-Parada, P. (2026). Beyond "Greenflation": Heterogeneous Price Dynamics in Critical Mineral Markets. *Revista Brasileira de Finanças*, *24*, e202601. https://doi.org/10.xxxx/xxxx
Submitted on January 1, 2026. Published online on March 31, 2026.
Editor in charge: Mr. Editor.
[†]marcelinolorenzo1805@usp.br
[‡]karine.borri@usp.br
[*]d.mesa@imperial.ac.uk
[**]p.brito-parada@imperial.ac.uk

1. Introduction

The growing number of studies addressing global environmental risks (such as biodiversity loss, ozone layer depletion, and climate instability (Geissdoerfer et al., 2017)) has prompted governments worldwide to seek strategies to combat climate threats and foster the energy transition. These initiatives include policy mechanisms such as zero-carbon certificates and tax exemptions for eco-friendly products (Hossain, 2024).

Among the alternatives, the increasing adoption of renewable energy sources (solar panels, wind turbines, and hydropower) has opened new perspectives and policy incentives for both industry and government. However, unlike traditional energy systems, emerging renewable technologies depend significantly more on critical metals throughout their supply chains.

The precise definition of a "critical mineral" is not a settled concept. Broadly, critical minerals encompass specific elements essential for low-emission and renewable technologies, used across different supply chain stages, from generation to distribution and storage (Månberger, 2021), including applications in computers, defense systems, battery storage, and mobile devices (Attílio, 2025). These minerals include copper, cobalt, lithium, nickel, and rare earth elements (REEs), which have gained increasing importance for the global transition to renewable energy (Grandell et al., 2016; Giurco et al., 2019; Church and Crawford, 2018).

Copper is fundamental for electrification infrastructure, acting through electricity transmission networks, battery storage, wind turbines, and second-generation solar photovoltaics (Elshkaki and Graedel, 2015). Lithium, cobalt, and nickel are essential for energy storage, being primary components of cathodes for lithium-ion batteries (International Energy Agency and Organisation for Economic Co-operation and Development, 2019). REEs are essential to electric vehicles and wind turbines (International Energy Agency, 2024a) due to their unique chemical properties, such as high magnetic strength and heat resistance (Golroudbary et al., 2022).

The continuous rise in demand for critical metals is projected to peak around 2030 (International Seabed Authority, 2022). Recent studies highlight that, under such conditions, the energy transition imposes exogenous demand shocks on mineral markets characterized by high dependency on these inputs. Previous estimations indicate that the total production value of metals, including lithium, cobalt, copper, and nickel, could quadruple to US$ 13 trillion between 2021 and 2040. This dynamic engenders the phenomenon of "greenflation," wherein metal price volatility acts as a cost transmission mechanism to renewable infrastructure (Boer et al., 2021).

Despite the recent momentum surrounding critical mineral extraction, few studies have empirically investigated their economic impacts, and little has been explored regarding how the renewable energy market is altering the price composition and structural dynamics of these metals (Soares et al., 2025; International Seabed Authority, 2022; Månberger, 2021; Schipper et al., 2018; Boer et al., 2024).

This paper investigates how energy transition drivers influence the pricing dynamics of copper and lithium under distinct market regimes, employing an SVAR identified via Non-Gaussian Maximum Likelihood (NGML). This novel method allows us to recover structurally independent shocks by exploiting the non-Gaussian information in the data, rather than imposing theoretical restrictions, providing a data-driven identification of contemporaneous spillovers without the risk of misspecification inherent in recursive ordering schemes.

Our results reveal a strong rejection of Gaussianity for both markets, validating the NGML approach. The US copper market exhibits rapid, difference-stationary adjustments to oil and bond yield shocks, consistent with the efficient market hypothesis. In contrast, the Chinese lithium market displays "hump-shaped" inertial responses in levels, reflecting structural rigidities and state-level intervention. We also identify a "productive slack" phenomenon in China, where renewable energy deployment paradoxically exerts negative pressure on lithium prices, contrasting with the cost-push inflation driven by coal prices.

Our findings suggest that the energy-mineral nexus operates through fundamentally distinct mechanisms depending on the institutional context of each market. In liberalized commodity markets, upstream cost pressures, rather than downstream renewable demand, appear to dominate critical mineral price formation in the short run. In state-directed economies, long-term deployment targets may effectively decouple mineral prices from conventional macroeconomic transmission channels. These results caution against uniform "greenflation" narratives.

This paper is organized as follows. Section 2 reviews the literature. Section 3 presents the methodology and data. Section 4 discusses the econometric results. Section 5 concludes and proposes future research.

2. Literature Review

Over the past three decades, growing concerns about climate change, environmental quality, and energy security have led academics and policymakers to reassess the use of traditional fossil fuels (Büyüközkan and Güleryüz, 2016; Aslan et al., 2022; Lin and Omoju, 2017). This shift toward photovoltaic solar

panels, energy storage batteries, wind turbines, and electric vehicles (EVs) implies a complex transformation of the global energy matrix (Månberger, 2021).

A primary strand of research focuses on physical supply constraints and material bottlenecks. Olivetti et al. (2017) analyzed the supply chains of key battery metals, particularly lithium and cobalt, over the 2002 to 2025 period, identifying potential bottlenecks that could hinder production scaling. Similarly, Tokimatsu et al. (2017) demonstrated that under aggressive transition scenarios, cumulative consumption of most critical metals threatens to exceed available reserves.

Complementing these physical balance approaches, econometric frameworks have been employed to estimate demand elasticities and the role of industrialization. Stuermer (2017) revealed significant heterogeneity across minerals: the long-run income elasticity of demand is below unity for tin, lithium, and zinc, whereas for copper it is close to one. More recently, Soares et al. (2025) applied an ARDL framework to project global copper demand up to 2030, incorporating GDP per capita and substitute prices.

A significant methodological leap was suggested by Attílio (2025), who reversed the traditional causality question by employing a Global Vector Autoregression (GVAR) to investigate how critical mineral price shocks impact the pace of the energy transition itself. His findings suggest that price spikes in metals like lithium and cobalt create negative spillovers that decelerate renewable adoption. However, while the GVAR framework effectively captures global inter-dependencies, its panel structure tends to impose homogeneity on transmission mechanisms, potentially overlooking the distinct idiosyncratic volatility and non-Gaussian shock distributions of specific commodity markets.

In summary, while existing literature has advanced understanding of physical constraints and demand projections, significant gaps remain. Most studies rely on reduced-form demand equations or standard VAR frameworks with Gaussian assumptions and recursive identification, approaches ill-suited for capturing the non-linear dynamics and contemporaneous interactions in volatile commodity markets. This paper addresses these gaps by employing SVAR-NGML, enabling data-driven recovery of structural shocks without arbitrary recursive orderings.

3. Methodology and Data

3.1 SVAR-NGML Specification

The Structural Vector Autoregression with Non-Gaussian Maximum Likelihood (SVAR-NGML) offers several advantages over conventional VAR approaches. It enables identification of structural shocks through non-Gaussianity without requiring controversial long-run or short-run restrictions (Lanne et al., 2017); accommodates heavy-tailed distributions and excess kurtosis commonly observed in metal and energy price series (Lütkepohl and Netšunajev, 2017); and proves robust to structural breaks and regime shifts (Herwartz and Plödt, 2016).

The foundation of our structural analysis is a reduced-form VAR of order p:

$$\mathbf{y}_t = \mathbf{c} + \sum_{j=1}^{p} \mathbf{A}_j \mathbf{y}_{t-j} + \mathbf{u}_t \tag{1}$$

where $\mathbf{y}_t$ is an $N \times 1$ vector of endogenous variables, $\mathbf{c}$ is an $N \times 1$ vector of intercepts, $\mathbf{A}_j$ are $N \times N$ coefficient matrices, and $\mathbf{u}_t$ is an $N \times 1$ vector of reduced-form residuals.

The relationship between reduced-form residuals $\mathbf{u}_t$ and structural shocks $\boldsymbol{\varepsilon}_t$ is given by:

$$\mathbf{u}_t = \mathbf{B}\boldsymbol{\varepsilon}_t \tag{2}$$

where $\mathbf{B}$ is the $N \times N$ contemporaneous impact matrix. The SVAR-NGML approach exploits the statistical properties of structural shocks for identification, assuming that shocks are mutually independent and that at most one follows a Gaussian distribution (Lanne et al., 2017; Lütkepohl and Netšunajev, 2017). This enables unique identification of $\mathbf{B}$ up to column permutations and sign changes.

The log-likelihood function under independent non-Gaussian structural shocks is:

$$\mathscr{L}(\mathbf{B}, \boldsymbol{\theta}) = \sum_{t=1}^{T} \left[\sum_{i=1}^{N} \log f_i(\varepsilon_{i,t}; \boldsymbol{\theta}_i) + \log |\det(\mathbf{B}^{-1})| \right] \tag{3}$$

We employ Student-t distributions for all structural shocks, where $\varepsilon_{i,t} \sim t_{\nu_i}$, to accommodate heavy-tailed behavior characteristic of commodity price innovations (Box, 1981; Lange et al., 2021).

Estimation proceeds in two stages: reduced-form VAR parameters are estimated by OLS, and the structural impact matrix **B** and degrees-of-freedom parameters $\{\nu_i\}$ are then recovered by maximum likelihood.[1] Statistical inference employs a residual-based bootstrap with 1,000 replications (Bertsche and Braun, 2022).

For the United States, we selected four lags, corresponding to a quarterly horizon in monthly data, and specify all variables in first differences. The China model employs two lags, twelve monthly seasonal dummies, a deterministic trend, and three exogenous dummies capturing the 2022 to 2023 lithium price collapse (International Energy Agency, 2024a), the 2020 to 2021 price surge, and the initial COVID-19 pandemic period (International Energy Agency, 2024b). Given persistent diagnostic failures under first-differencing for the China model, we follow Sims et al. (1990) and adopt a levels specification.

3.2 Variables

The generalized endogenous vector is defined as:

$$\mathbf{y}_t = [Metal_t,\ REN_t,\ Fossil_t,\ Bond_t,\ Ind_t] \tag{4}$$

For the United States, the system comprises:

$$\mathbf{y}_t^{USA} = \left[Cu_t,\ REN_t^{USA},\ Oil_t,\ Bond_t,\ Ind_t\right] \tag{5}$$

capturing copper prices (Cu_t), renewable energy capacity additions (REN_t^{USA}), crude oil prices (Oil_t), ten-year government bond yields ($Bond_t$), and industrial production (Ind_t). The US possesses a mature, highly liquid copper futures market and significant domestic reserves, ranking as the fifth-largest global producer (U.S. Geological Survey, 2024).

For China, the system comprises:

$$\mathbf{y}_t^{China} = \left[Lithium_t,\ Ren_t^{China},\ Coal_t,\ M2_t,\ Ind_t\right] \tag{6}$$

China processes approximately 65% of the world's lithium and manufactures over 75% of global lithium-ion batteries (International Energy Agency, 2024a). Coal prices ($Coal_t$) replace oil to reflect coal's dominant role in China's energy mix, and money supply ($M2_t$) replaces bond yields to capture state-led credit expansion channels.

[1] The SVAR estimation, NGML identification, IRFs, and FEVDs were performed using R software (version 2025.09.2+418, package 'svars').

Table 1
Descriptive statistics and data sources

				Descriptive Statistics					
Variable	**Unit**	**Exchange**	**Period**	**Mean**	**SD**	**Min**	**Max**	**Skew**	**Kurt**
Panel A: United States Model									
Copper (*Cu*)	USD/mt (Log)	IMF	2012 to 2025	9.031	0.159	8.707	9.394	0.042	2.414
Renewable Prod. (REN_{US})	GW	IEA	2012 to 2025	11.046	0.256	10.474	11.605	0.055	2.199
Crude Oil (*Oil*)	USD/bbl (Log)	EIA US	2012 to 2025	4.381	0.319	3.046	4.972	0.299	4.170
Ind. Prod. (Ind_{US})	Index (12/2005=100)	LSEG	2012 to 2025	4.699	0.029	4.526	4.733	2.599	14.375
Long Term Rate US (*Bond*)	m.g %	FRED	2012 to 2025	2.501	1.008	0.620	4.800	0.435	2.532
Panel B: China Model									
Lithium (*Li*)	USD/mt (Log)	IMF	2015 to 2025	11.800	0.491	11.317	13.173	1.307	3.934
Renewable Prod. (REN_{CH})	GW	IEA	2015 to 2025	12.077	0.336	11.179	12.743	0.172	2.358
Coal (*Coal*)	USD/mt (Log)	IMF	2015 to 2025	4.712	0.561	3.939	6.148	0.885	3.297
Money Supply (*M2*)	m.g %	IMF	2015 to 2025	9.839	1.888	6.200	14.000	0.255	2.131
Ind. Prod. (Ind_{CH})	Index (12/2005=100)	LSEG	2015 to 2025	4.668	0.039	4.460	4.906	0.734	18.213

Note: IMF: International Monetary Fund Commodity Price System; EIA US: Energy Information Administration; IEA: International Energy Agency; LSEG: London Stock Exchange Group.

Table 1 presents the descriptive statistics, data sources, and sample periods for all variables. The US model spans May 2012 to May 2025 and the China model spans January 2015 to May 2025, with the difference due to data availability constraints.[2] All price series are expressed in real terms (May 2025 base), deflated using the Producer Price Index (PPI) from the Federal Reserve.

3.3 Treatment of Nonstationarity and Cointegration

Preliminary diagnostic tests confirm that most variables follow an $I(1)$ process, with the exception of renewable energy capacity, which is stationary in levels ($I(0)$) (see Table A2 in Appendix A).

Table 2 summarizes the Johansen cointegration test results (Johansen, 1991). Panel A reports the trace statistics for the United States model. We strongly reject the null hypothesis of no cointegrating relationship at all relevant ranks through $r \leqslant 3$ (trace statistic of 195.29 against a 5% critical value of 76.07 for $r = 0$), with the test accepting H_0 only at $r \leqslant 4$ (trace statistic of 3.80 below the critical value of 7.52). This indicates the presence of four cointegrating vectors. Despite this evidence of long-run relationships, the first-differenced specification for the US model remains appropriate, as the stationarity transformation absorbs the common stochastic trends and ensures valid short-run inference.

Panel B presents the results for the Chinese economy. The test fails to reject the null hypothesis of no cointegration at the 5% level, with a trace statistic of 74.61 falling marginally below the critical value of 76.07 ($p = 0.064$). While this borderline result warrants caution, strict adherence to the conventional significance threshold precludes the use of a Vector Error Correction Model (VECM). Notably, the proximity to the threshold is consistent with the near-

[2] As a robustness check, the US model was estimated over the restricted 2015 to 2025 sample; structural results remained qualitatively unchanged.

integrated dynamics of China's lithium market documented in the stability diagnostics, where the maximum inverse root of 0.994 approaches but does not breach unity. In both models, therefore, the SVAR specification is the appropriate framework: for the US, because the first-differenced variables are stationary and the analysis targets short-run shock transmission; for China, because formal cointegration is not established at conventional levels. In both cases, the SVAR ensures that the analysis remains centred on volatility spillovers and contemporaneous adjustment mechanisms, which aligns with our core research objectives.

Although the US cointegrating vectors could in principle be examined for economic interpretation, the SVAR in first differences remains the appropriate framework for our short-run analysis. For China, the statistical acceptance of $r = 0$ confirms the absence of a stable long-run equilibrium over the sample period, consistent with the levels specification adopted for that model.

Table 2
Johansen Fisher cointegration test results

Panel A: United States Model (Trace Statistic)

Hypothesis	Eigenvalue	Trace Stat	Crit. 5%	Crit. 1%	Result
None ($r = 0$)	0.3578	195.29	76.07	84.45	Reject H_0
At most 1 ($r \leqslant 1$)	0.3070	128.40	53.12	60.16	Reject H_0
At most 2 ($r \leqslant 2$)	0.2495	73.00	34.91	41.07	Reject H_0
At most 3 ($r \leqslant 3$)	0.1573	29.65	19.96	24.60	Reject H_0
At most 4 ($r \leqslant 4$)	0.0248	3.80	7.52	9.24	Accept H_0

Panel B: China Model (Trace Statistic)

Hypothesis	Eigenvalue	Trace Stat	Crit. 5%	Crit. 1%	Result
None ($r = 0$)	0.2508	74.61	76.07	84.45	Accept H_0
At most 1 ($r \leqslant 1$)	0.1544	39.67	53.12	60.16	Accept H_0
At most 2 ($r \leqslant 2$)	0.0953	19.38	34.91	41.07	Accept H_0

Note: Critical values sourced from (MacKinnon et al., 1999). For Panel A, rejection of H_0 implies the presence of cointegrating relationships.

4. Results

4.1 Regression Estimates

The coefficients from the VAR estimations are reported in Tables 3 and 4, revealing distinct structural dynamics regarding how power markets and macroeconomic conditions drive critical mineral prices.

For the United States (Table 3), copper prices exhibit a clear dual-stage behavior. In the first lag, prices are positively driven by their own momentum

Table 3
Short-run VAR Estimations from United States

	Lag Order (Coefficients)			
Regressor	$t-1$	$t-2$	$t-3$	$t-4$
Copper (Δ)	0.234***	-0.008	-0.081	0.089
	(0.089)	(0.090)	(0.091)	(0.091)
Renewables	0.050	-0.056	-0.083	0.105**
	(0.045)	(0.060)	(0.060)	(0.044)
Crude Oil (Δ)	0.088*	-0.098*	-0.015	-0.042
	(0.046)	(0.050)	(0.050)	(0.048)
Bond Yield (Δ)	-0.032	0.042*	-0.037	0.006
	(0.022)	(0.023)	(0.023)	(0.021)
Ind. Prod. (Δ)	-0.345	0.704**	-0.421	0.063
	(0.335)	(0.354)	(0.357)	(0.319)
Constant	-0.181 (0.164)			
Diagnostic Statistics				
Resid. Std. Error: 0.042	Adj. R^2: 0.090		F-stat: 1.742 (p=0.034)	

Notes: Standard errors in parentheses. Dependent variable: $\Delta copper$. $^{***}p < 0.01$, $^{**}p < 0.05$, $^{*}p < 0.1$.

(0.234***) and crude oil prices (0.088*), consistent with oil serving as a high-frequency proxy for aggregate demand. Copper behaves primarily as a financial asset at this stage, responding to global liquidity before physical constraints bind. By the second lag, drivers shift toward the real economy (Soares et al., 2025): industrial production exerts a positive impact (0.704**), and bond yields show a positive coefficient (0.042*), consistent with a demand-pull scenario.

Notably, the relationship with crude oil turns negative (−0.098*) at the second lag, suggesting a structural substitution effect as the demand for electrification infrastructure intensifies. Finally, renewable energy deployment exhibits a significant positive impact at the fourth lag (0.105**), reflecting the maturation of the supply chain whereby cumulative renewable capacity translates into sustained structural demand for copper in grid infrastructure.

The Chinese model (Table 4) reveals a highly volatile market driven primarily by autoregressive behavior and structural shocks. The lithium price is heavily influenced by its own lag with conflicting magnitudes, suggesting market overreaction: a strong positive effect at lag one (1.334***) is sharply corrected at lag two (−0.439***). This "boom-bust" signature reflects an immature market prone to speculative bubbles followed by rapid corrections (Martin et al., 2017). The significant positive relationship between coal and lithium (0.095**) suggests that lithium refining remains tethered to the coal-based energy complex despite decarbonization goals.

Table 4
Short-run VAR Estimations from China

Regressor	Lag $t-1$	Lag $t-2$
Autoregressive Terms		
Lithium	1.334*** (0.066)	-0.439*** (0.064)
Renewables	-0.169** (0.074)	0.104 (0.075)
Coal	0.095** (0.045)	-0.007 (0.046)
Money Supply	-0.003 (0.008)	0.005 (0.008)
Ind. Prod.	-0.111 (0.145)	-0.094 (0.147)
Deterministic Terms & Structural Breaks		
Constant	2.545*** (0.714)	
Recent Crash (Dummy)	-0.147*** (0.052)	
Bubble Rally (Dummy)	0.261*** (0.039)	
Past Structural (Dummy)	0.235*** (0.051)	
Seasonal Controls (Monthly Dummies)		
SD_1 (Jan)	-0.004 (0.025)	
SD_2 (Feb)	0.025 (0.025)	
SD_3 (Mar)	-0.019 (0.023)	
SD_4 (Apr)	0.012 (0.034)	
SD_5 (May)	-0.006 (0.025)	
SD_6 (Jun)	0.056* (0.029)	
SD_7 (Jul)	0.009 (0.027)	
SD_8 (Aug)	0.038 (0.029)	
SD_9 (Sep)	0.017 (0.024)	
SD_{10} (Oct)	0.018 (0.023)	
SD_{11} (Nov)	0.031 (0.025)	
Diagnostic Statistics		
Resid. Std. Error: 0.047	Adj. R^2: 0.991	F-stat: 557.9***

Notes: Standard errors in parentheses. Dependent variable: *lithium* (log-levels). Seasonal dummies SD_1–SD_{11} control for monthly fixed effects (December is base). ***, **, * denote significance at 1%, 5%, and 10%.

4.2 Structural Identification and Contemporaneous Spillovers

Table 5 presents the systematic comparison between NGML and the conventional Cholesky decomposition. Both models exhibit substantially elevated empirical kurtosis values (10.97 and 12.08 for the US and China, respectively), significantly exceeding the Gaussian benchmark of 3.00. Formal normality tests reject Gaussianity in both specifications ($p < 0.001$), validating the NGML framework.

Panel B demonstrates systematic improvements in model fit when relaxing the Gaussianity restriction. For the US, the NGML approach achieves a log-likelihood of 1,204.85 compared to 1,144.71 under Cholesky, with a

Likelihood Ratio statistic of 120.28 rejecting the Gaussian restriction at the 1% level. The China model yields log-likelihood values of 765.89 and 659.67 for NGML and Cholesky, respectively, with an LR statistic of 212.45 ($p < 0.001$).

Panel C confirms that NGML achieves statistical independence among structural shocks without imposing arbitrary zero restrictions. Maximum absolute correlations between identified shocks remain negligible (0.0337 and 0.0722 for the US and China models, respectively), validating the core identifying assumption.

Table 5
Structural identification: NGML vs. Cholesky

	USA Copper Model		China Lithium Model	
Criterion	**NGML**	**Cholesky**	**NGML**	**Cholesky**
Panel A: Distributional Properties				
Kurtosis Assumption	Non-Gaussian	Gaussian	Non-Gaussian	Gaussian
Avg. Empirical Kurtosis	10.97	–	12.08	–
Normality Test (p-val)	$< 0.001^{***}$	Assumed	$< 0.001^{***}$	Assumed
Distribution Spec.	Student-t	Normal	Student-t	Normal
Panel B: Model Fit Statistics				
Log-Likelihood	1204.85	1144.71	765.89	659.67
AIC	–	–	–	–
BIC	–	–	–	–
LR Test Statistic	120.28^{***}	–	212.45^{***}	–
Panel C: Shock Independence				
Independence Test	Satisfied***	Imposed	Satisfied***	Imposed
Max Correlation ($\lvert\rho\rvert$)	0.0337	0.0000	0.0722	0.0000

Notes: ***, **, * denote significance at 1%, 5%, and 10%. LR test compares NGML (unrestricted) against Cholesky; strongly rejects Cholesky restrictions ($p = 0.000$).

Table 6 reports the estimated contemporaneous impact matrix (B). For the US (Panel A), copper displays a moderate contemporaneous volatility impact (0.0286). Notably, copper and industrial production exhibit a significant negative spillover (-0.0244^{***}), suggesting that positive production shocks temporarily depress copper prices through increased scrap supply. Oil shocks contemporaneously affect industrial production (0.0097^{***}) and bond yields (0.0165). For China (Panel B), the negative and statistically significant spillover from lithium prices to renewable energy deployment (-0.0234^{**}) suggests that abrupt lithium price increases immediately constrain renewable investment through elevated battery storage costs. The estimated intrinsic volatility of China's money supply shocks (0.5875) substantially exceeds that observed in the US specification for the long-term rate (0.1491), potentially reflecting differences in monetary transmission between state-directed and

market-oriented economies.

Table 6
Contemporaneous impact matrix (B): NGML identification

Panel A: USA Copper Model					
Variable ↓ / Shock →	**Copper**	**Renew.**	**Oil**	**Bond**	**Ind.Prod.**
Copper	**0.0286*****	0.0058	0.0021	-0.0124	-0.0244***
Renewable (USA)	0.0006	**0.0731*****	-0.0006	0.0181	0.0192*
Oil	-0.0195	0.0078	**0.0507*****	0.0165	-0.0656***
Bond Yield	0.0538	-0.0088	0.0044	**0.1491*****	-0.0682**
Ind. Production	0.0017*	0.0001	0.0097***	0.0000	**0.0025*****
Panel B: China Lithium Model					
Variable ↓ / Shock →	**Lithium**	**Renew.**	**Coal**	**Bond**	**Ind.Prod.**
Lithium	**0.0471*****	-0.0089	0.0067	-0.0034	0.0012
Renewable (CN)	-0.0234**	**0.0610*****	-0.0023	-0.0045	0.0034
Coal	0.0123	-0.0012	**0.0972*****	-0.0067	-0.0023
Money Supply	-0.0345	-0.0167	-0.0089	**0.5875*****	-0.0056
Ind. Production	0.0023	0.0045	-0.0034	-0.0012	**0.0323*****

Notes: ***, **, * denote significance at 1%, 5%, and 10% based on two-tailed Z-tests. Diagonal elements (bold) represent the immediate impact of a structural shock on its own variable. Matrix B is identified via NGML without zero restrictions.

4.3 Impulse Response Function Results

Figure 1 presents the structural impulse response functions for the United States model, tracing the dynamic effects of one-standard-deviation shocks on copper prices over a 24-month horizon, with 68% bootstrap confidence intervals.

The immediate response of copper prices to an idiosyncratic copper shock (Panel a) registers at approximately -4%. The confidence band remains statistically distinguishable from zero only through the first to second month, confirming rapid market absorption consistent with supply-demand clearing mechanisms (Ryter et al., 2025).

Panel (b) reveals a statistically significant but modest positive transmission from renewable energy deployment shocks, with an initial negative peak of approximately 1.8% from the first to third month; the confidence band converges toward zero after the first to second month. Panel (c) shows a subtle negative relationship between oil price shocks and copper prices (-1.5% at initial impact), with significance confined to the first to second month. The cost-push channel dominates at short horizons: higher fossil fuel prices squeeze mining profitability and dampen investment in copper-intensive projects, before

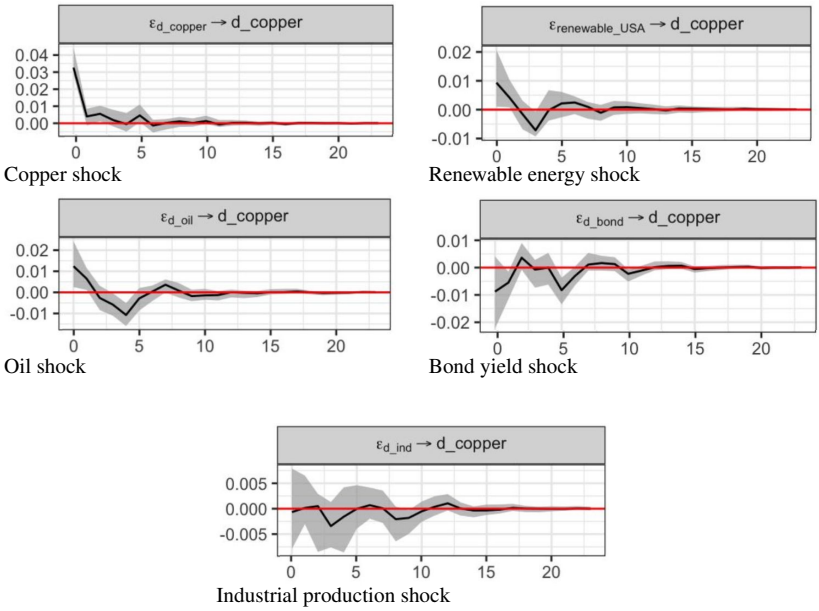

Figure 1
Structural impulse response functions for the copper model. Shaded bands are 68% bootstrap confidence intervals (1,000 replications).

longer-run substitution effects materialize (Jiang et al., 2025).

Panels (d) and (e) document statistically insignificant responses. Bond yield shocks generate a modest oscillatory pattern reaching approximately 2% by the third month, but the 68% confidence band encompasses zero throughout the entire 24-month horizon. Industrial production shocks exhibit a V-then-U-shaped pattern with oscillations of approximately $\pm 0.5\%$ through the fifth month, followed by a shallower 0.2% U-shaped recovery through the tenth month; confidence bands likewise encompass zero throughout.

In contrast, Figure 2 presents the structural impulse response functions for the Chinese lithium market. A striking feature is the pronounced hump-shaped trajectory of the responses, indicating significant structural rigidities distinct from the volatility adjustments observed in the US model.

Panel (a) reveals a high degree of persistence in the response of lithium prices to their own shock. Following an initial surge of 0.5% in the first month, the price level exhibits a slow, inertial decay, returning to equilibrium only after approximately ten months. The 68% confidence band remains statistically

distinguishable from zero throughout the full 24-month horizon, reflecting the highly persistent nature of own-price shocks in this state-mediated market. This "soft landing" likely reflects the efficacy of state-managed production quotas and strategic inventory releases (Wang et al., 2023).

Panel (b) presents a counter-intuitive but structurally sound result: renewable energy deployment shocks exert a significant negative impact on lithium prices, reaching a trough of -2.7% around the seventh month. The 68% confidence band remains distinguishable from zero through approximately the eighth to ninth month. This negative transmission reflects the centralized planning of China's energy matrix, where a shock to renewable energy demand signals a simultaneous state-directed expansion of lithium extraction and refinery activities, leading to a deliberate build-up of idle capacity. The expectation of a supply glut outweighs the immediate demand effect, depressing prices. Our results suggest that China actively mitigates the risk identified by Attílio (2025) through a "security-via-saturation" strategy.

Panel (c) shows that coal price shocks follow an upward U-shaped pattern across the full 24-month horizon, with a price spike of almost 10% in the seventh month. The 68% confidence band remains statistically distinguishable from zero throughout all 24 months, reflecting the deep structural integration between coal prices and lithium production costs in China (Jiang et al., 2025; Balashova and Serletis, 2020).

Panels (d) and (e) confirm that money supply shocks and industrial production shocks exert no statistically significant influence on lithium prices at any horizon. This finding reinforces the interpretation that lithium price dynamics in China are driven primarily by idiosyncratic supply-side shocks, coal-driven cost pressures, and renewable energy deployment policy, rather than by cyclical macroeconomic fluctuations. This mechanism reflects "policy forward guidance" under China's state-led capitalism: by establishing rigid long-term targets for the energy transition, the state preemptively anchors producer expectations, effectively isolating the critical mineral market from traditional monetary transmission mechanisms.

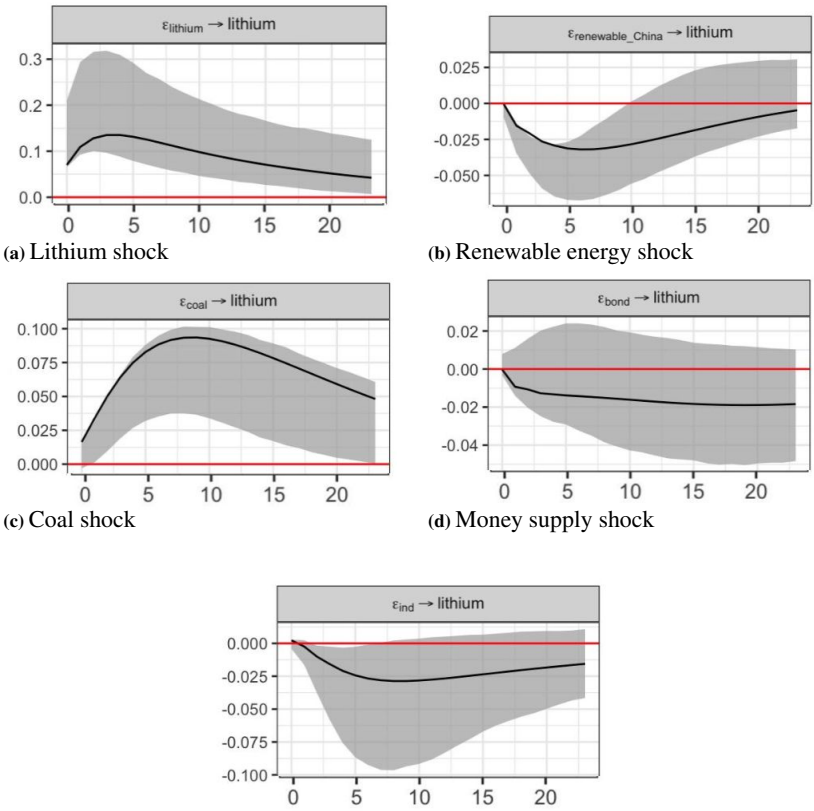

(a) Lithium shock
(b) Renewable energy shock
(c) Coal shock
(d) Money supply shock
(e) Industrial production shock

Figure 2
Structural impulse response functions for the lithium model. Shaded bands are 68% bootstrap confidence intervals (1,000 replications).

4.4 Variance Decomposition

Figure 3 presents the forecast error variance decomposition (FEVD) for copper prices in the US. The results exhibit a notably diversified variance composition, with own-shock copper contributions accounting for approximately 40 to 50% of forecast error variance across the 24-month horizon, while structural shocks originating outside the copper market collectively account for 55 to 65% of total variance.

Renewable energy demand shocks contribute approximately 4 to 6% to

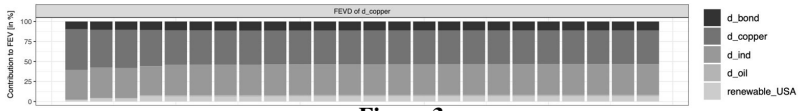

Figure 3
Forecast error variance decomposition for copper prices.

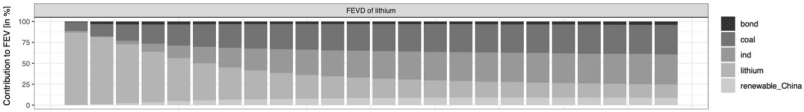

Figure 4
Forecast error variance decomposition for lithium prices.

copper price forecast error variance. Oil price shocks represent a negligible influence at approximately 0.5 to 1% of variance contribution, reaffirming the negative and insignificant contemporaneous relationship documented in the IRF. Bond yield shocks contribute approximately 12.5% to variance, capturing the influence of monetary condition changes on commodity inventory valuations and mining investment decisions (Hotelling, 1931). Industrial production shocks exhibit an expressive variance of approximately 36%, reflecting the relationship between real economy dynamics and copper prices over the horizon.

Figure 4 presents the FEVD for lithium prices in China. The results exhibit persistent own-shock dominance: idiosyncratic lithium price shocks account for approximately 65 to 70% of forecast error variance from one month ahead through the fifth month, declining to around 28 to 18% over the year projection.

Renewable energy demand shocks stabilize at approximately 7.5 to 9% of lithium price forecast error variance after the third month, reflecting the direct and intensive linkage between China's planned expansion of renewable energy and lithium production. Coal price shocks contribute approximately 25 to 30% to variance by the second month, representing the most significant external contributor and challenging simplistic narratives of lithium as a direct coal substitute, instead pointing to nuanced cost-input transmission channels. Money supply shocks contribute only 2 to 4% to lithium price variance, confirming that state-directed credit expansion operates through sectoral allocation mechanisms rather than broad price-level effects. Industrial production shocks account for approximately 25 to 30% of lithium price forecast error variance, appearing significantly from the third month onward.

5. Conclusions

This study investigates the heterogeneous transmission mechanisms of energy transition shocks on copper and lithium prices in the United States and China, employing an SVAR identified via NGML. Our findings reveal a stark dichotomy between these two critical mineral markets, challenging the assumption of a uniform "greenflation" effect.

In the US model, copper behaves as a mature and globally integrated upstream commodity. Copper prices display rapid adjustments to structural shocks, driven predominantly by cost-push factors, specifically crude oil prices and bond yields, rather than downstream demand-pull mechanisms like domestic renewable energy deployment or industrial production. In stark contrast, the Chinese lithium market exhibits pronounced structural inertia to broad macroeconomic aggregates. The mechanism of "policy forward guidance" under China's state-led capitalism anchors producer expectations through long-term deployment targets, decoupling mineral prices from traditional short-term neoclassical price theory. Complementarily, the FEVD reveals that coal price shocks are a dominant contributor to lithium price variance, highlighting a complex cost-input dependency: lithium extraction and processing remain highly energy-intensive and partially tethered to coal-fired electricity.

These asymmetric findings offer critical implications for policymakers. Copper and lithium respond to identical energy transition drivers through fundamentally different mechanisms, implying that uniform policy prescriptions will generate inefficient outcomes. For market economies, policies must address the transitional bottleneck of upstream costs through subsidized exploration, streamlined permitting, or strategic stockpiling. For policymakers engaging with state-directed economies, securing supply chains requires understanding that competition with China involves robust, long-term forward guidance to anchor domestic producer expectations.

Several limitations qualify these conclusions. First, the sample period encompasses multiple structural breaks, including China's 2015 stock market crisis, the COVID-19 pandemic, and the 2022 energy crisis, that more sophisticated regime-switching models could better capture. Second, this study does not formally model the role of financial market sentiment and forward-looking financial proxies in the expectation channel, a critical frontier for future research. Third, our focus on price dynamics abstracts from quantity adjustments in physical markets; integrating consumption and inventory data would provide a more complete picture of market equilibrium responses. Fourth, the bilateral US-China framework neglects other major producing countries, particularly Chile and Australia for lithium and copper, respectively. Multi-country network

models could reveal additional transmission channels.

Despite these limitations, this research demonstrates that the energy transition will not generate uniform commodity price pressures. Critical mineral markets will evolve along divergent trajectories shaped by institutional characteristics, industrial organization, and policy regimes.

References

Aslan, A. et al. (2022). Renewable energy and economic growth relationship under the oil reserve ownership: evidence from panel var approach, *Renewable Energy*, *188*, 402–410.

Attílio, L. A. (2025). Impact of critical mineral prices on energy transition, *Applied Energy*, *377*, 124688.

Balashova, S. and Serletis, A. (2020). Oil prices shocks and the russian economy, *The Journal of Economic Asymmetries*, *21*, e00148.

Bertsche, D. and Braun, R. (2022). Identification of structural vector autoregressions by stochastic volatility, *Journal of Business & Economic Statistics*, *40*(1), 328–341.
URL: https://ideas.repec.org/a/taf/jnlbes/v40y2022i1p328-341.html

Boer, L., Pescatori, A. and Stuermer, M. (2021). Energy transition metals, *IMF Working Papers*, *2021*(243).

Boer, L., Pescatori, A. and Stuermer, M. (2024). Energy transition metals: Bottleneck for net-zero emissions?, *Journal of the European Economic Association*, *22*(1), 200–229. Previously circulated as IMF Working Paper 2021/243.

Box, J. F. (1981). Gosset, fisher, and the t distribution, *The American Statistician*, *35*(2), 61–66.
URL: http://www.jstor.org/stable/2683142

Büyüközkan, G. and Güleryüz, S. (2016). An integrated dematel-anp approach for renewable energy resources selection in turkey, *International Journal of Production Economics*, *182*, 435–448.

Church, C. and Crawford, A. (2018). Green conflict minerals: The fuels of conflict in the transition to a low-carbon economy, *Technical report*, International Institute for Sustainable Development (IISD).

Elshkaki, A. and Graedel, T. E. (2015). Solar cell metals and their hosts: A tale of oversupply and undersupply, *Applied Energy*, *158*, 167–177.

Geissdoerfer, M., Savaget, P., Bocken, N. M. P. and Hultink, E. J. (2017). The circular economy – a new sustainability paradigm?, *Journal of Cleaner Production*, *143*, 757–768.

Giurco, D. et al. (2019). Requirements for minerals in a clean energy transition, *Resources, Conservation and Recycling*, *145*.

Golroudbary, S. R. et al. (2022). Global environmental cost of using rare earth elements in green energy technologies, *Science of The Total Environment*, *832*, 155022.

Grandell, L. et al. (2016). Role of critical metals in the future markets of clean energy technologies, *Renewable Energy*, *95*, 53–62.

Hamilton, J. D. (1994). *Time Series Analysis*, Princeton University Press, Princeton, NJ. The standard reference for VAR stability conditions (Unit Circle).

Herwartz, H. and Plödt, M. (2016). Simulation evidence on theory-based and statistical identification under volatility breaks, *Oxford Bulletin of Economics and Statistics*, *78*(1), 85–112.
URL: https://doi.org/10.1111/obes.12098

Hossain, M. (2024). The feasibility of flexible and adaptive green certification in accelerating zero carbon cities, *Environmental Development*, *52*, 101091.

Hotelling, H. (1931). The economics of exhaustible resources, *Journal of Political Economy*, *39*(2), 137–175.
URL: http://www.jstor.org/stable/1822328

International Energy Agency (2024a). Global critical minerals outlook 2024, *Technical report*, IEA, Paris.
URL: https://www.iea.org/reports/global-critical-minerals-outlook-2024

International Energy Agency (2024b). Global critical minerals outlook 2024, *Technical report*, IEA, Paris.
URL: https://www.iea.org/reports/global-critical-minerals-outlook-2024

International Energy Agency and Organisation for Economic Co-operation and Development (2019). *Global EV Outlook 2019: Scaling-up the Transition to Electric Mobility*, OECD Publishing, Paris.

URL: https://www.oecd-ilibrary.org/energy/global-ev-outlook-2019_35fb60bd-en

International Seabed Authority (2022). Deep-sea minerals and the green economy, *Technical report*, ISA, Kingston.

Jarque, C. M. and Bera, A. K. (1987). A test for normality of observations and regression residuals, *International Statistical Review*, *55*(2), 163–172. Seminal paper for the JB Normality Test.

Jiang, Z. et al. (2025). Impact of oil prices on key energy mineral prices: Fresh evidence from quantile and wavelet approaches, *Energy Economics*, *145*, 108461.

Johansen, S. (1991). Estimation and hypothesis testing of cointegration vectors in gaussian vector autoregressive models, *Econometrica*, *59*(6), 1551–1580.
URL: http://www.jstor.org/stable/2938278

Lange, A., Dalhaus, T., Lütkepohl, H. and Netsunajev, A. (2021). Identification of structural vector autoregressions by stochastic volatility, *Journal of Economic Dynamics and Control*, *122*, 104029.

Lanne, M., Meitz, M. and Saikkonen, P. (2017). Identification and estimation of non-gaussian structural vector autoregressions, *Journal of Econometrics*, *196*(2), 288–304.

Lin, B. and Omoju, O. E. (2017). Focusing on the right targets: economic factors driving non-hydro renewable energy transition, *Renewable Energy*, *113*, 52–63.

Lütkepohl, H. and Netšunajev, A. (2017). Structural vector autoregressions with smooth transition in variances, *Journal of Economic Dynamics and Control*, *84*, 43–57.

MacKinnon, J. G., Haug, A. A. and Michelis, L. (1999). Numerical distribution functions of likelihood ratio tests for cointegration, *Journal of Applied Econometrics*, *14*(5), 563–577.
URL: https://ideas.repec.org/a/jae/japmet/v14y1999i5p563-77.html

Månberger, A. (2021). Critical minerals and great power competition, *Technical report*, Stockholm International Peace Research Institute (SIPRI).

Martin, G., Rentsch, L., Höck, M. and Bertau, M. (2017). Lithium market research – global supply, future demand and price development, *Energy*

Storage Materials, *6*, 171–179.
URL: https://doi.org/10.1016/j.ensm.2016.11.004

Olivetti, E. A., Ceder, G., Gaustad, G. G. and Fu, X. (2017). Lithium-ion battery supply chain considerations: Analysis of potential bottlenecks in critical metals, *Joule*, *1*(2), 229–243.

Ryter, J., Bhuwalka, K., Roth, R., Olivetti, E., Buarque-Andrade, L., Frenzel, M., Shojaeddini, E., Alonso, E. and Nassar, N. (2025). Modeling interconnected minerals markets with multicommodity supply curves: examining the copper-cobalt-nickel system, *Nature Communications*, *16*(1), 7302.
URL: https://doi.org/10.1038/s41467-025-62570-8

Schipper, B. W., Lin, H.-C., Meloni, M. A., Wansleeben, K., Heijungs, R. and van der Voet, E. (2018). Estimating global copper demand until 2100 with regression and stock dynamics, *Resources, Conservation and Recycling*, *132*, 28–36.

Sims, C. A., Stock, J. H. and Watson, M. W. (1990). Inference in linear time series models with some unit roots, *Econometrica*, *58*(1), 113–144. Justifies estimating VAR in levels when cointegration is present.

Soares, A. F., Spers, R. G. and Santos Jhunior, R. d. O. (2025). Projection of global copper demand in the context of energy transition, *Resources Policy*, *91*, 105567.
URL: https://doi.org/10.1016/j.resourpol.2025.105567

Stuermer, M. (2017). Industrialization and the demand for mineral commodities, *Journal of International Money and Finance*, *76*, 16–27.

Tokimatsu, K., Murakami, S., Adachi, T., Ii, R., Yasuoka, R. and Nishio, M. (2017). Long-term demand and supply of non-ferrous mineral resources by a mineral balance model, *Mineral Economics*, *30*(3), 193–206.

U.S. Geological Survey (2024). Mineral commodity summaries 2024, *Technical report*, U.S. Geological Survey, Reston, VA.
URL: https://pubs.usgs.gov/periodicals/mcs2024/mcs2024.pdf

Wang, X. et al. (2023). Bubble behaviors in lithium price and the contagion effect, *Resources Policy*, *85*, 103846.

A. Preliminary Diagnostic Testing

Table A1 presents the diagnostic tests and stability conditions for both specifications. Panel A confirms that the stability condition is satisfied for both models, as all inverse characteristic roots lie within the unit circle (Hamilton, 1994). A comparative analysis reveals a structural divergence: while the United States model exhibits rapid convergence (0.718), the Chinese model displays high persistence (0.994), approximating the unit root threshold. Regarding residual normality (Panel B), the Jarque-Bera test (Jarque and Bera, 1987) strongly rejects the null hypothesis for both models ($p < 0.01$), supporting the NGML identification strategy (Lanne et al., 2017). Panel C confirms the absence of serial correlation and conditional heteroskedasticity.

Table A1
VAR residual diagnostic tests and stability conditions

	USA (Copper)		China (Lithium)	
Diagnostic Test	**Stat.**	**p-val**	**Stat.**	**p-val**
Panel A: Stability Condition				
Max. Inv. Root	0.718	–	0.994	–
Conclusion	Stable (< 1)		Stable (< 1)	
Panel B: Normality (Jarque-Bera)				
Joint JB Test	1,383.7	0.00***	5,037	0.00***
Skewness	153.53	0.00***	157	0.00***
Kurtosis	1230.2	0.00***	4,880	0.00***
Panel C: Serial Corr. & Heterosk.				
Portmanteau	313.3	0.0558	605.4	0.051
ARCH-LM	2,085	0.5074	1,665	1.000

Notes: *** $p < 0.01$. Portmanteau (Adj.): USA (12 lags), CN (24 lags). H_0: No serial corr. ARCH-LM (Multivar.): 12 lags. H_0: Homoscedasticity. Normality rejected; NGML strategy adopted.

Table A2
Unit root and stationarity tests

	Level (Log)		1st Diff. (Δ)		
Variable	**ADF**	**PP**	**ADF**	**PP**	**Dec.**
Panel A: United States Model					
Copper (*Cu*)	-2.77	-8.56	-12.4***	-12.5***	$I(1)$
Crude Oil (*Oil*)	-2.15	-11.31	-11.3***	-11.1***	$I(1)$
Ind. Prod. (*Ind*)	-2.75	-21.56	-8.55***	-8.60***	$I(1)$
Renewables (REN^{USA})	-8.15***	-61.1***	–	–	$I(0)$
Bond Yield (*Bond*)	-1.44	-4.48	-9.87***	-9.91***	$I(1)$
Panel B: China Model					
Lithium (*Li*)	-2.07	-3.20	-3.20**	-9.91***	$I(1)$
Coal (*Coal*)	-2.30	-5.52	-10.3***	-10.4***	$I(1)$
Ind. Prod. (*Ind*)	-2.76	-61.42	-7.92***	-7.95***	$I(1)$
Renewables (REN^{China})	-11.9***	-48.8***	–	–	$I(0)$
Money Supply ($M2$)	-2.13	-8.06	-10.4***	-10.4***	$I(1)$

Notes: ***, ** denote significance at 1% and 5%. ADF: Augmented Dickey-Fuller; PP: Phillips-Perron.